

Fluid Turbulence in Quantum Plasmas

Dastgeer Shaikh*

Institute of Geophysics and Planetary Physics, University of California, Riverside, California 92521, USA

P. K. Shukla†

*Institut für Theoretische Physik IV, Ruhr-Universität Bochum, D-44780 Bochum, Germany,
and School of Physics, University of KwaZulu-Durban, Durban 4000, South Africa*

(Received 19 February 2007; published 19 September 2007)

Nonlinear fluid simulations are developed by us to investigate the properties of fully developed two-dimensional (2D) electron fluid turbulence in a very dense Fermi (quantum) plasma. We find that a 2D quantum electron plasma exhibits dual cascades, in which the electron number density cascades towards smaller turbulent scales, while the electrostatic potential forms larger scale eddies. The characteristic turbulent spectrum associated with the nonlinear electron plasma oscillations (EPO) is determined critically by a ratio of the energy density of the EPOs and the electron kinetic energy density of quantum plasmas. The turbulent transport corresponding to the large-scale potential distribution is predominant in comparison with the small-scale electron number density variation, a result that is consistent with the classical diffusion theory.

DOI: 10.1103/PhysRevLett.99.125002

PACS numbers: 52.27.Gr, 52.35.Ra

About 45 years ago, Pines [1] had laid down the foundation for quantum plasma physics. During the last decade, there has been a growing interest in investigating new aspects of dense quantum plasmas by developing the quantum hydrodynamic (QHD) equations [2] by incorporating the quantum force associated with the Bohm potential [2], by deriving the Child-Langmuir law in the quantum regime [3], and by studying numerous collective effects [4–7] involving different quantum forces (e.g., due to the Bohm potential [2] and the pressure law [4,5] for the Fermi plasma, as well as the potential energy of the electron-1/2 spin magnetic moment in a magnetic field [8]). Studies of collective interactions in dense quantum plasmas are relevant for the next generation intense laser-solid density plasma experiments [9,10], for superdense astrophysical bodies [11,12] (e.g., the interior of white dwarfs and neutron stars), as well as for micro- and nano-scale objects (e.g., quantum diodes [3], quantum dots and nanowires [13], and nanophotonics [14]).

The Wigner-Poisson (WP) model [15] has been used to derive a set of QHD equations [4,5] for a dense electron plasma. The QHD equations include the continuity, momentum and Poisson equations. The quantum nature [4] appears in the electron momentum equation through the pressure term, which requires the knowledge of the Wigner distribution for a quantum mixture of electron wave functions, each characterized by an occupation probability. The quantum part of the electron pressure is represented as a quantum force [2,4] $-\nabla\phi_B$, where $\phi_B = -(\hbar^2/2m_e\sqrt{n_e})\nabla^2\sqrt{n_e}$, \hbar is the Planck constant divided by 2π , m_e is the electron mass, and n_e is the electron number density. Defining the effective wave function $\psi = \sqrt{n_e(\mathbf{r}, t)}\exp[iS(\mathbf{r}, t)/\hbar]$, where $\nabla S(\mathbf{r}, t) = m_e\mathbf{u}_e(\mathbf{r}, t)$ and $\mathbf{u}_e(\mathbf{r}, t)$ is the electron velocity, the electron momentum equation can be represented as an effective nonlinear

Schrödinger (NLS) equation [4,5,7], in which there appears a coupling between the wave function and the electrostatic potential associated with the electron plasma oscillations (EPOs). The electrostatic potential is determined from the Poisson equation. We thus have the coupled NLS and Poisson equations, which govern the dynamics of nonlinearly interacting EPOs in a dense quantum plasmas. This mean-field model of Refs. [4,5] is valid to the lowest order in the correlation parameter, and it neglects correlations between electrons. The density functional theory [16] incorporates electron-electron correlations, which are neglected in the present Letter.

In this Letter, we use the coupled NLS and Poisson equations for investigating, by means of computer simulations, the properties of 2D electron fluid turbulence and associated electron transport in quantum plasmas. We find that the nonlinear coupling between the EPOs of different scale sizes gives rise to small-scale electron density structures, while the electrostatic potential cascades towards large-scales. The total energy associated with our quantum electron plasma turbulence, nonetheless, possesses a characteristic spectrum, which is a *non*-Kolmogorov-like. The electron diffusion caused by the electron fluid turbulence is consistent with the dynamical evolution of turbulent mode structures.

For our 2D turbulence studies, we use the nonlinear Schrödinger-Poisson equations [4,7]

$$i\sqrt{2H}\frac{\partial\Psi}{\partial t} + H\nabla^2\Psi + \varphi\Psi - |\Psi|^2\Psi = 0, \quad (1)$$

and

$$\nabla^2\varphi = |\Psi|^2 - 1, \quad (2)$$

which are valid at zero electron temperature for the Fermi-Dirac equilibrium distribution, and which govern the dy-

namics of nonlinearly interacting EPOs of different wavelengths. In Eqs. (1) and (2) the wave function Ψ is normalized by $\sqrt{n_0}$, the electrostatic potential φ by $k_B T_F/e$, the time t by the electron plasma period ω_{pe}^{-1} , and the space \mathbf{r} by the Fermi Debye radius λ_D . We have introduced the notations $\lambda_D = (k_B T_F/4\pi n_0 e^2)^{1/2} \equiv V_F/\omega_{pe}$ and $\sqrt{H} = \hbar\omega_{pe}/\sqrt{2}k_B T_F$, where k_B is the Boltzmann constant and the Fermi electron temperature $k_B T_F = (\hbar^2/2m_e) \times (3\pi^2)^{1/3} n_0^{2/3}$, e is magnitude of the electron charge, and $\omega_{pe} = (4\pi n_0 e^2/m_e)^{1/2}$ is the electron plasma frequency. The origin of the various terms in Eq. (1) is obvious. The first term is due to the electron inertia, the H -term in (1) is associated with the quantum tunneling involving the Bohm potential, $\varphi\Psi$ comes from the nonlinear coupling between the scalar potential (due to the space charge electric field) and the electron wave function, and the cubic nonlinear term is the contribution of the electron pressure [4] for the Fermi plasma that has a quantum statistical equation of state. We are using the CGS units throughout this Letter.

Equations (1) and (2) admit a set of conservation laws [8], including the number of electrons $N = \int \Psi^2 dx dy$, the electron momentum $\mathbf{P} = -i \int \Psi^* \nabla \Psi dx dy$, the electron angular momentum $\mathbf{L} = -i \int \Psi^* \mathbf{r} \times \nabla \Psi dx dy$, and the total energy $\mathcal{E} = \int [-\Psi^* H \nabla^2 \Psi + |\nabla \varphi|^2/2 + |\Psi|^3/2] dx dy$. In obtaining the total energy \mathcal{E} , we have used the relation $\partial \mathbf{E}/\partial t = iH(\Psi \nabla \Psi^* - \Psi^* \nabla \Psi)$, where the electric field $\mathbf{E} = -\nabla \varphi$. The conservations laws are used to maintain the accuracy of the numerical integration of Eqs. (1) and (2), which hold for quantum electron-ion plasmas with fixed ion background. The assumption of immobile ions is valid, since the EPOs (given by the dispersion relation [4,5] $\omega^2 = \omega_{pe}^2 + k^2 V_F^2 + \hbar^2 k^4/4m_e^2$) occur on the electron plasma period, which is much shorter than the ion plasma period ω_{pi}^{-1} . Here ω and k are the frequency and the wave number, respectively. The ion dynamics, which may become important in the nonlinear phase on a longer time scale (say of the order of ω_{pi}^{-1}), in our investigation can easily be incorporated by replacing 1 in Eq. (2) by n_i , where the normalized (by n_0) ion density n_i is determined from $d_t n_i + n_i \nabla \cdot \mathbf{u}_i = 0$ and $d_t \mathbf{u}_i = -C_s^2 \nabla \varphi$, where $d_t = (\partial/\partial t) + \mathbf{u}_i \cdot \nabla$, \mathbf{u}_i is the ion velocity, $C_s = (k_B T_F/m_i)^{1/2}$ is the ion sound speed, and m_i is the ion mass.

The nonlinear mode coupling interaction studies are performed to investigate the multiscale evolution of a decaying 2D electron fluid turbulence, which is described by Eqs. (1) and (2). All the fluctuations are initialized isotropically (no mean fields are assumed) with random phases and amplitudes in Fourier space, and evolved further by the integration of Eqs. (1) and (2), using a fully de-aliased pseudospectral numerical scheme [17] based on the Fourier spectral methods. The spatial discretization in our 2D simulations uses a discrete Fourier representation of turbulent fluctuations. The numerical algorithm employed here conserves energy in terms of the dynamical fluid

variables and not due to a separate energy equation written in a conservative form. The evolution variables use periodic boundary conditions. The initial isotropic turbulent spectrum was chosen close to k^{-2} , with random phases in all directions. The choice of such (or even a flatter than -2) spectrum treats the turbulent fluctuations on an equal footing and avoids any influence on the dynamical evolution that may be due to the initial spectral nonsymmetry. The equations are advanced in time using a 4th order Runge-Kutta (RK4) scheme. The code is made stable by a proper de-aliasing of spurious Fourier modes, and by choosing a relatively small time step in the simulations. Our code is massively parallelized using message passing interface libraries to facilitate higher resolution in a 2D computational box, with a resolution of 512^2 grid points.

We study the properties of 2D fluid turbulence, composed of nonlinearly interacting EPOs, for two specific physical systems. These are the dense plasmas in the next generation laser-based plasma compression (LBPC) schemes [10] as well as in superdense astrophysical objects [11,12] (e.g., white dwarfs). It is expected that in LBPC schemes, the electron number density may reach 10^{27} cm^{-3} and beyond. Hence, we have $\omega_{pe} = 1.76 \times 10^{18} \text{ s}^{-1}$, $k_B T_F = 1.7 \times 10^{-9} \text{ erg}$, $\hbar\omega_{pe} = 1.7 \times 10^{-9} \text{ erg}$, and $H = 1$. The Fermi Debye length $\lambda_D = 0.1 \text{ \AA}$. On the other hand, in the interior of white dwarfs, we typically have [18] $n_0 \sim 10^{30} \text{ cm}^{-3}$ (such values are also common in dense neutron stars and supernovae), yielding $\omega_{pe} = 5.64 \times 10^{19} \text{ s}^{-1}$, $k_B T_F = 1.7 \times 10^{-7} \text{ erg}$, $\hbar\omega_{pe} = 5.64 \times 10^{-8} \text{ erg}$, $H \simeq 0.03$, and $\lambda_D = 0.025 \text{ \AA}$. The numerical solutions of Eqs. (1) and (2) for $H = 1$ and $H = 0.025$ (corresponding to $n_0 = 10^{27} \text{ cm}^{-3}$ and $n_0 = 10^{30} \text{ cm}^{-3}$, respectively) are displayed in Fig. 1, which are the electron number density and electrostatic (ES) potential distributions in the (x, y) plane.

Figure 1 reveals that the electron density distribution has a tendency to generate smaller length-scale structures, while the ES potential cascades towards larger scales. The coexistence of the small and larger scale structures in turbulence is a ubiquitous feature of various 2D turbulence systems. For example, in 2D hydrodynamic turbulence, the incompressible fluid admits two invariants, namely, the energy and the mean squared vorticity. The two invariants, under the action of an external forcing, cascade simultaneously in turbulence, thereby leading to a dual cascade phenomena. In these processes, the energy cascades towards longer length scales, while the fluid vorticity transfers spectral power towards shorter length scales. Usually, a dual cascade is observed in a driven turbulence simulation, in which certain modes are excited externally through random turbulent forces in spectral space. The randomly excited Fourier modes transfer the spectral energy by conserving the constants of motion in k space. On the other hand, in freely decaying turbulence, the energy contained in the large-scale eddies is transferred to

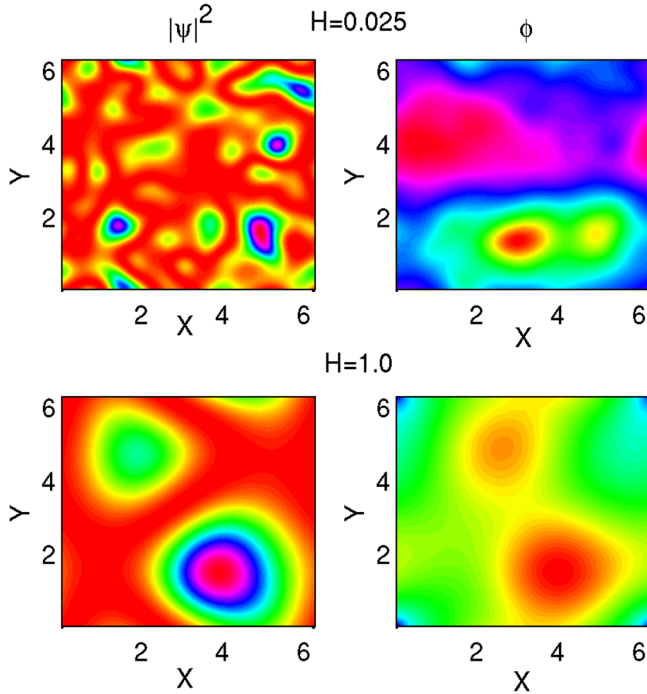


FIG. 1 (color online). Small scale fluctuations in the electron density resulted from our steady turbulence simulations of 2D electron Fermi plasma. Forward cascades are responsible for the generation of small-scale fluctuations. Large scale structures are present in the electrostatic potential, essentially resulting from an inverse cascade.

the smaller scales, leading to a statistically stationary inertial regime associated with the forward cascades of one of the invariants. Decaying turbulence often leads to the formation of coherent structures as turbulence relaxes, thus making the nonlinear interactions rather inefficient when they are saturated. The power spectrum exhibits an interesting feature in our 2D electron plasma system, unlike the 2D hydrodynamic turbulence [19,20]. The spectral slope in the 2D quantum electron fluid turbulence is close to the Iroshnikov-Kraichnan (IK) power law [21,22] $k^{-3/2}$, rather than the usual Kolomogrov power law [19] $k^{-5/3}$. We further find that this scaling is not universal and is determined critically by the quantum tunneling parameter H . For instance, for a higher value of $H = 1.0$ the spectrum becomes more flat (see Fig. 2). Furthermore, for $H = 0.65$ one encounters a turbulence spectrum that decays as k^{-1} (not shown in the Fig. 2). Physically, the flatness (or deviation from the $k^{-5/3}$), is likely to result from the short wavelength part of the EPOs spectrum which is controlled by the quantum tunneling effect H associated with the Bohm potential. The peak in the energy spectrum can be attributed to the higher turbulent power residing in the EPO potential, which eventually leads to the generation of larger scale structures, as the total energy encompasses both the electrostatic potential and electron density components. In our dual cascade process, there is a delicate competition

between the EPO dispersions caused by the statistical pressure law (giving the $k^2 V_F^2$ term, which dominates at longer scales) and the quantum Bohm potential (giving the $\hbar^2 k^4 / 4m_e^2$ term, which dominates at shorter scales with respect to a source). Furthermore, it is interesting to note that exponents other than $k^{-5/3}$ have also been observed in numerical simulations [23] of the Charney and 2D incompressible Navier-Stokes equations.

We finally estimate the electron diffusion coefficient in the presence of small and large-scale turbulent EPOs in 2D quantum plasma. An effective electron diffusion coefficient caused by the momentum transfer can be calculated from $D_{\text{eff}} = \int_0^\infty \langle \mathbf{P}(\mathbf{r}, t) \cdot \mathbf{P}(\mathbf{r}, t + t') \rangle dt'$, where \mathbf{P} is the electron momentum and the angular brackets denotes spatial averages and the ensemble averages are normalized to unit mass. Since the 2D structures are confined to an x - y plane, the effective electron diffusion coefficient, D_{eff} , essentially relates the diffusion processes associated with random translational motions of the electrons in nonlinear plasmonic fields. We compute D_{eff} in our simulations, to measure the turbulent electron transport that is associated with the turbulent structures we have reported herein. It is observed that the effective electron diffusion is lower when the field perturbations are Gaussian. On the other hand, the electron diffusion increases rapidly with the eventual formation of longer length-scale structures, as shown in Fig. 3. The electron diffusion due to large-scale potential distributions in quantum plasmas dominates substantially, as

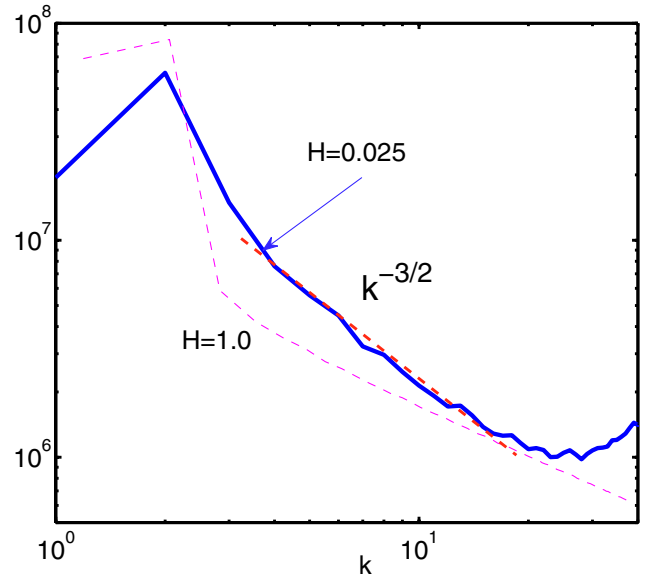


FIG. 2 (color online). Small-scale fluctuations in the electron density coexisting with the large scale electrostatic potential structures lead to an inertial range power spectrum which is determined critically by H (ratio of the energy density of the EPOs and the electron kinetic energy density of quantum plasmas). The 2D electron fluid turbulence interestingly relaxes towards an IK type $k^{-3/2}$ spectrum in a dense Fermi plasma for $H = 0.025$.

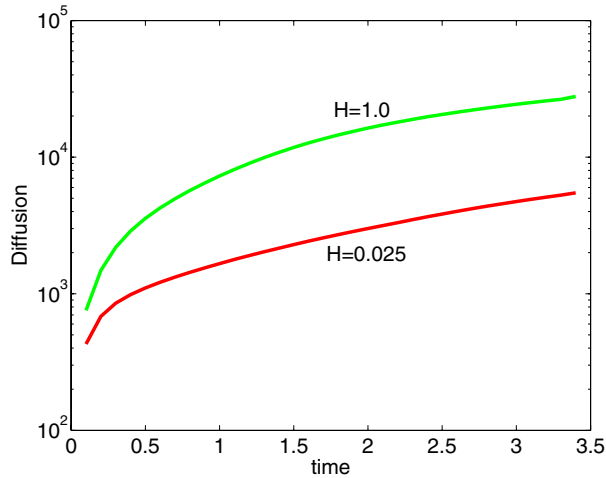


FIG. 3 (color online). Time evolution of an effective electron diffusion coefficient corresponds to the diffusion associated with the large-scale electrostatic potential and the small-scale electron density. Here a comparison between $H = 1$ and $H = 0.025$ is shown.

depicted in Fig. 3. Furthermore, in the steady state, nonlinearly coupled EPOs form stationary structures, and D_{eff} saturates eventually. Thus, remarkably an enhanced electron diffusion results primarily due to the emergence of large-scale potential structures in our 2D quantum plasma.

In summary, we have presented computer simulation studies of the 2D fluid turbulence in a dense quantum plasma. Our simulations, for the parameters that are representative of the next generation intense laser-solid density plasma experiments as well as of the superdense astrophysical bodies, reveal new features of the dual cascade in a fully developed 2D electron fluid turbulence. Specifically, we find that the power spectrum associated with nonlinearly interacting EPOs in quantum plasmas follow a non-Kolmogorov-like IK spectrum for $H = 0.025$. However, for higher values of H there appears a deviation from the IK spectrum. It turns out that the scaling exponent is sensitive to the variation of H , which represents the ratio between the energy density of EPOs and the electron kinetic energy density in dense quantum plasmas. In conclusion, we have identified new fluid turbulence aspects of very dense 2D quantum plasmas in which finite

amplitude EPOs are nonlinearly interacting in a complex fashion.

*dastgeer@ucr.edu

†ps@tp4.rub.de

- [1] D. Pines, J. Nucl. Energy, Part C, Plasma Phys. Accel. Thermonucl. Res. **2**, 5 (1961).
- [2] C.L. Gardner and C. Ringhofer, Phys. Rev. E **53**, 157 (1996).
- [3] L. K. Ang *et al.*, Phys. Rev. Lett. **91**, 208303 (2003); L. K. Ang and P. Zhang, *ibid.* **98**, 164802 (2007).
- [4] G. Manfredi and F. Haas, Phys. Rev. B **64**, 075316 (2001).
- [5] G. Manfredi, Fields Inst. Commun. **46**, 263 (2005).
- [6] F. Haas, Phys. Plasmas **12**, 062117 (2005).
- [7] P. K. Shukla and B. Eliasson, Phys. Rev. Lett. **96**, 245001 (2006).
- [8] M. Marklund and G. Brodin, Phys. Rev. Lett. **98**, 025001 (2007).
- [9] G. Mourou *et al.*, Rev. Mod. Phys. **78**, 309 (2006); Y. A. Salamin *et al.*, Phys. Rep. **427**, 41 (2006).
- [10] V.M. Malkin *et al.*, Phys. Rev. E **75**, 026404 (2007).
- [11] G. Chabrier *et al.*, J. Phys. Condens. Matter **14**, 9133 (2002); J. Phys. A **39**, 4411 (2006).
- [12] A.K. Harding and D. Lai, Rep. Prog. Phys. **69**, 2631 (2006).
- [13] G.V. Shpatakovskaya, J. Exp. Theor. Phys. **102**, 466 (2006).
- [14] W.L. Barnes *et al.*, Nature (London) **424**, 824 (2003); D.E. Chang *et al.*, Phys. Rev. Lett. **97**, 053002 (2006).
- [15] E. P. Wigner, Phys. Rev. **40**, 749 (1932); M. Hillery *et al.*, Phys. Rep. **106**, 121 (1984).
- [16] P. Hohenberg and W. Kohn, Phys. Rev. **136**, B864 (1964); W. Kohn and L.J. Sham, Phys. Rev. **140**, A1133 (1965); L. Brey *et al.*, Phys. Rev. B **42**, 1240 (1990).
- [17] D. Gottlieb and S.A. Orszag, *Numerical Analysis of Spectral Methods* (SIAM, Philadelphia, 1977).
- [18] I. Iben, Jr. and A.V. Tutukov, Astrophys. J. **282**, 615 (1984).
- [19] A. N. Kolmogorov, C.R. Acad. Sci. USSR **30**, 301 (1941).
- [20] M. Lesieur, *Turbulence in Fluids* (Kluwer, Dordrecht, 1990); U. Frisch, *Turbulence* (Cambridge University Press, Cambridge, England, 1995).
- [21] P. Iroshnikov, Sov. Astron. **7**, 566 (1963).
- [22] R.H. Kraichnan, Phys. Fluids **8**, 1385 (1965).
- [23] V.D. Larichev and J.C. McWilliams, Phys. Fluids A **3**, 938 (1991); R.K. Scott, Phys. Rev. E **75**, 046301 (2007).